CONTACT FATIGUE PROPAGATION OF DEEP DEFECTS IN RAILWAY WHEELS

S.Beretta[1], G.Donzella[2], R.Roberti[2], A. Ghidini[3]

[1] Dipartimento di Meccanica, Politecnico di Milano
Piazza Leonardo da Vinci 32, 20133 Milano (Italy)
[2] Dipartimento di Ingegneria Meccanica, Università di Brescia
Via Branze 38, 25123 Brescia (Italy)
[3] Lucchini Siderurgica S.p.A., via Paglia 45, 24065 Lovere (Italy)

ABSTRACT

Several different damage phenomena may occur in railway wheels: surface wear, pitting and generally surface contact fatigue, spalling and subsurface crack propagation under mode I and mode II. In an ideal description of the fatigue process (i.e. in the case of an initial defect-free material), cracks mainly nucleate under the action of shear stresses; stress based criteria, especially those considering a critical plane approach can be used to predict crack nucleation.

However, defects inherent in the wheel material or produced by the manufacturing process can strongly affect the different damage mechanisms and their importance in determining the life of the in service wheels. Deep defects in particular are difficult to be detected and can lead to severe spalling and this peculiar mechanism of damage has not been completely understood yet.

In this work the propagation mechanism of this kind of deep spalling has been assessed by experimental fractography, statistical analysis of inclusions, simulation of manufacturing process and FEM analysis of crack propagation. Some peculiarities of this damage mechanism have been evidenced, showing different stages in crack evolution.

INTRODUCTION

Several different damage phenomena may occur in railway wheels: surface wear, pitting and generally surface contact fatigue, spalling and subsurface crack propagation under mixed modes [1,2]. In an ideal description of the fatigue process (i.e. in the case of an initial defect-free material), cracks mainly nucleate under the action of shear stresses; stress based criteria, especially those considering a critical plane approach can be therefore used to predict crack nucleation [3].

However, defects inherent in the wheel material or produced by the manufacturing process can strongly affect the different damage mechanisms and their importance in determining the life of the in service wheels. Deep defects in particular are difficult to be detected and can lead to severe spalling and this peculiar mechanism of damage has not been completely understood yet.

Several attempt have been made in the past to assess the dangerous effect of subsurface micro and macro defects under rolling contact fatigue [4,5,6,7]. However, most of these studies consider plane models for the SIFs calculation and consequently are not able to correctly describe of an elliptical inclusion. The typical problem of these solutions is that there is no direct relationship between the shape of observed

defects and the initial size of the 2-D crack. A few studies (see for example [8,9]) deal with 3D defects and, because of the problem complexity, the solutions are unfortunately only valid for the specific applications examined.

The scope of this paper is to highlight the peculiarities of 'deep spalling' failures. The fractographic examination of these type of failures shows that they originates from narrow clusters of aluminate inclusions. The investigations carried out have shown that this type of defect is not consistent with the inherent defects of the matrix and FEM simulation have shown that the defects are due to the manufacturing process.

The most important point is that the observation shows that, in spite of simple 2-D analysis which consider a mode II propagation, the crack growth can be divided in different phases. The initial defect changes its shape up to a penny-shape crack and only in the final stage it propagates under mode II. The problem is complex because of the simultaneous presence of all the three modes of propagation, which can be partially or totally activated by the contact stresses.

In this paper an approximated approach is presented, which is however able to put in evidence the effect of the different modes in the crack propagation, thus justifying the experimental observations.

'DEEP SPALLING' FAILURES OF RAILWAY WHEELS

Material of the wheels

The steel grade used for the fabrication of the wheels complies with specification for R7 steel given by UIC Leaflet 812-3 [10]. The steel is melted in an electric arc furnace and then refined and vacuum degassed in an ASEA-SKF ladle furnace. The steel work process improves micro homogeneity and micro purity of the steel.

During heat treatment the solid wheels are given a rim chilling, i.e. only the rim is cooled with water in order to build up tangential compression stresses in the wheel rim. According to the low hardenability of the steel, martensitic transformation is limited to a thin layer that is machined out during finishing. The microstructure of the steel consists of almost equiaxed ferrite and pearlite grains. This type of microstructure is proven to give the best behaviour during service in terms of wear resistance.

'Deep spalling' fractures

The typical appearance of one of the failures that we call deep 'spalling' is shown in Fig. 1. These failures, even if their occurrence is very low (a few cases in the last 10 years), have been studied because of their peculiar mechanism.

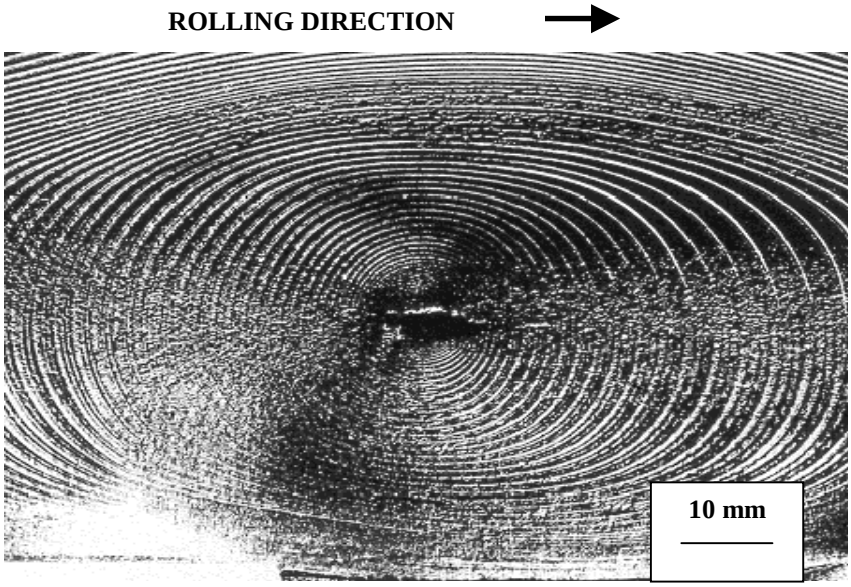

Figure 1: Typical appearance of 'deep spalling' failures: crack propagation is parallel to the rolling surface.

The fracture consists of a fatigue crack propagation surface parallel to the external surface of the wheel that leads to the detachment of a 'tile' with a length of a few hundreds of millimetres. At the origin of fracture there are inclusions of Al_2O_3 platelets elongated in the rolling direction. The typical dimensions of the original defects have a length of 1-5 mm and a width of 0.3-1 mm.
This type of failure appears only on high speed trains after reprofiling the worn wheel: the typical depth at which the defects occur is between 10 and 15 mm. This peculiar damage of the wheel can be extremely severe, especially considering its typical depth, since it can strongly affect the dynamic behaviour of wheels in high speed trains.

Origin of defects

In order to understand the origin of the clustered particles that cause the formation of 'deep spalling' two types of analyses were carried out.

The first investigation was done for that are present in the material of the wheels. The analysis was carried out by using the method of polished sections on material samples directly cut from the external region of wheels. The polished section revealed that the defects and inhomogeneities that can be found are constituted by two main types: sulphides and $Al_2O_3(CaO)_x$ particles. The latter are in particular the largest ones (Fig. 2).

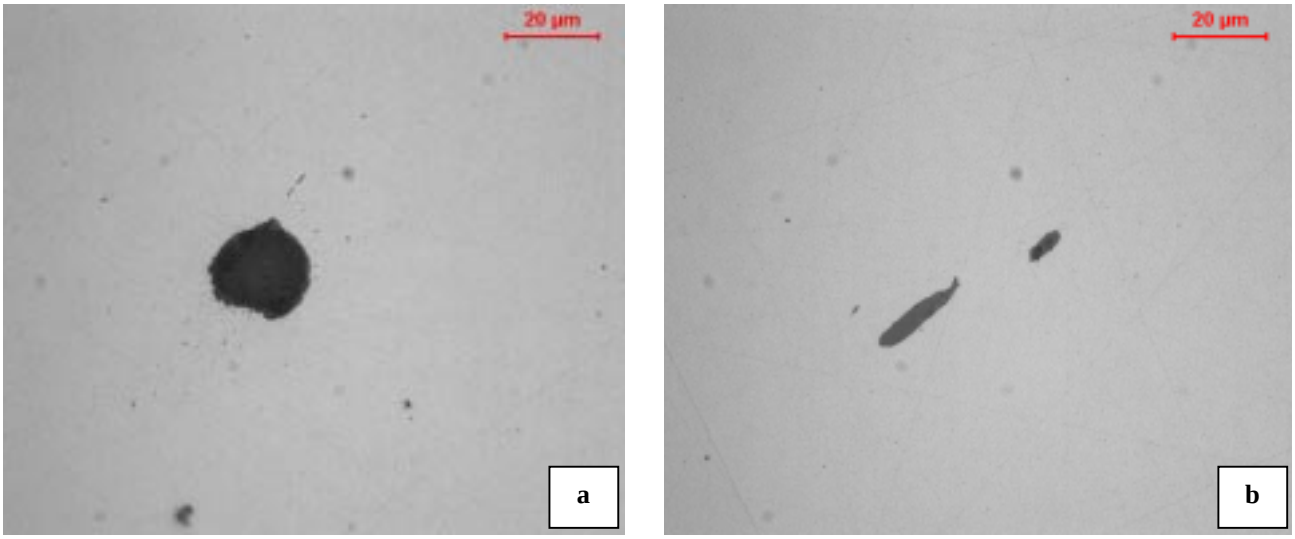

Figure 2: Typical defects that are found in the wheel material: a) an $Al_2O_3(CaO)_x$ particle; b) a Mn sulphide.

The quantitative analysis of defects was carried out by adopting the so-called 'extreme value inclusion rating' [11]. The two types of inclusions were sampled by taking the maximum defects on control areas So=0.76 mm^2. The data so obtained were then analysed with the Largest Extreme Value distribution in order to estimate the characteristic dimension of the maximum defect in a volume corresponding to the zone where failures occur (V= $5 \cdot 10^6$ mm^3). The maximum defects resulted respectively to be about 100 µm.

It can be immediately noticed that the extreme defect pertaining to particles 'inherently' present in the material are very different from the defects at the fracture origin. Because of this fact it was decided to carry out a FEM simulation of the plastic deformation of the wheel. The simulation of the deformation process, whose details can be found in [12], has been has then been followed backwards.

Figure 3.a shows the location of the defect in the finished part: the point has been singled out by means of the "marked-point". The backwards simulation has shown the position of the initial defect at the end of the pre-deformation (Fig. 3.b) and within the starting workpiece (Fig. 3.c).
Figure 3.d shows the effective strain at the end of the deformation process. Since the location of the defect is in correspondence of a high strain gradient within the workpiece it may be expected that an original non metallic inclusion is broken and deformed into a larger defect during the deformation.

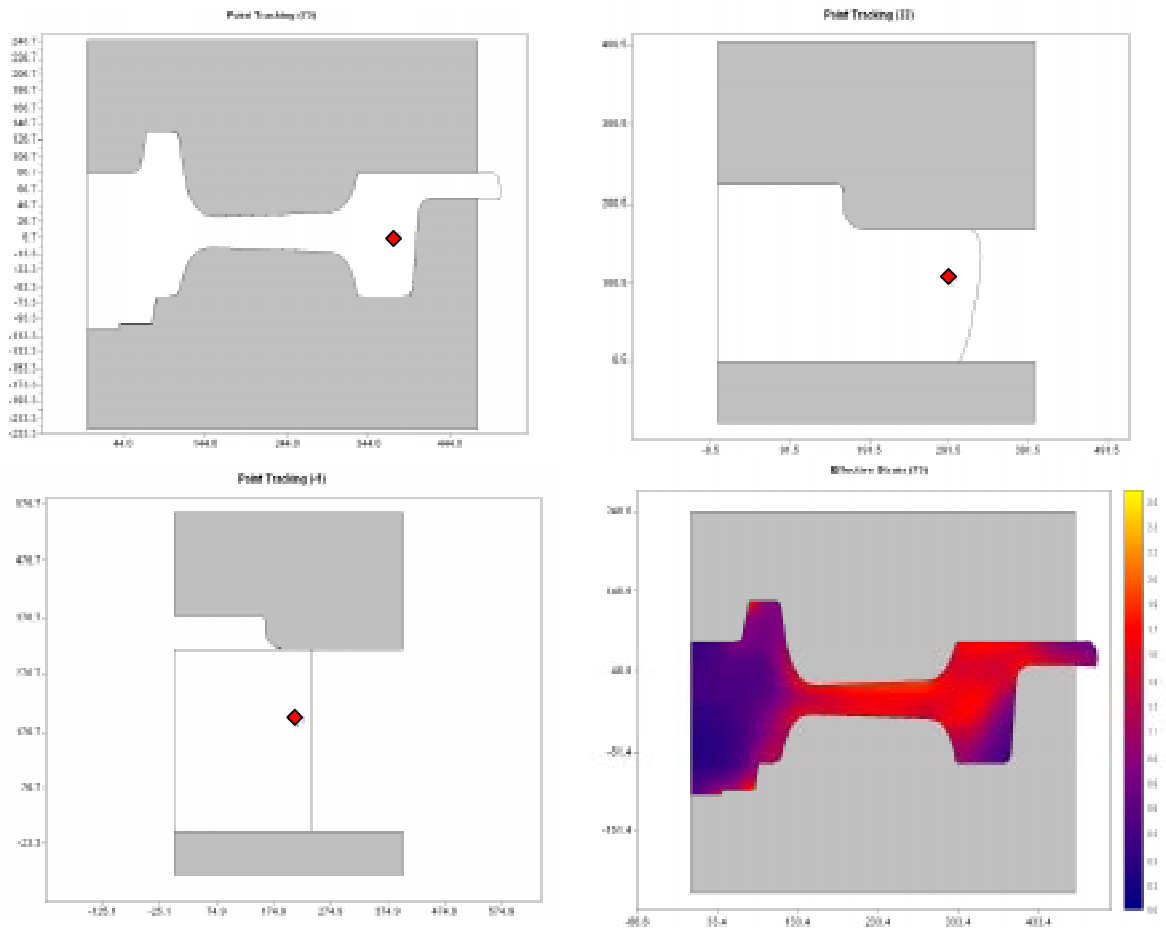

Figure 3: Simulation of plastic deformation of the wheel : a-c) backwards locations of the defect (♦) in the finished part ; d) map of effective strains at the end of plastic process.

FRACTOGRAPHY

The fracture surfaces of the few 'deep spalling' fractures have been examined under SEM in order to investigate the common aspects of fracture propagation. The first remark is that in all the cases the fracture originate from a narrow inclusion almost elliptical (typical shape ratio a/b=0.2). Tracking the markings on fracture surface it can be seen that the propagation consists of two phases (Fig. 4).

Firstly the initial defect propagates in a direction perpendicular to rolling thus changing its shape and it eventually tends to become a penny-shape crack. After this stage, the fracture grows mainly in the rolling direction, this propagation being presumably sustained by shear stresses.

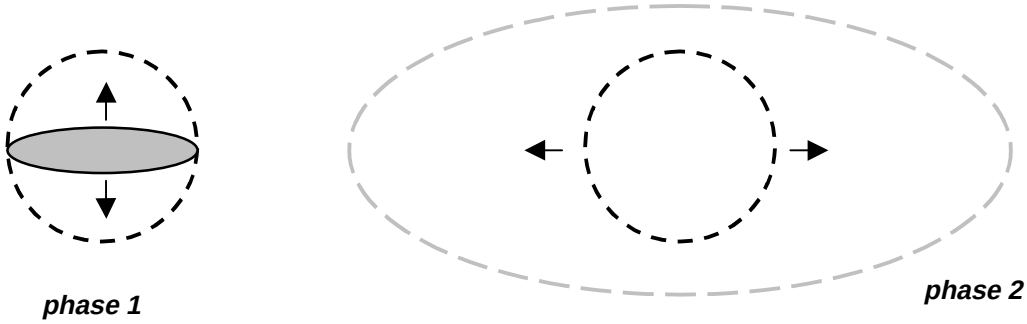

Figure 4: The two phases of propagation of fractures in deep spalling.

The fractographic observations confirm that, in the region corresponding to first stages of *phase 1*, the propagation is markedly different from the fracture surface in the other regions. Morover the fracture surface in zones corresponding to *phase 2* are similar to mode II propagation surfaces of recent experiments by Murakami et al. [13]. Figure 5 shows the evidences of these different propagation regimes for the defect shown in Fig. 1.

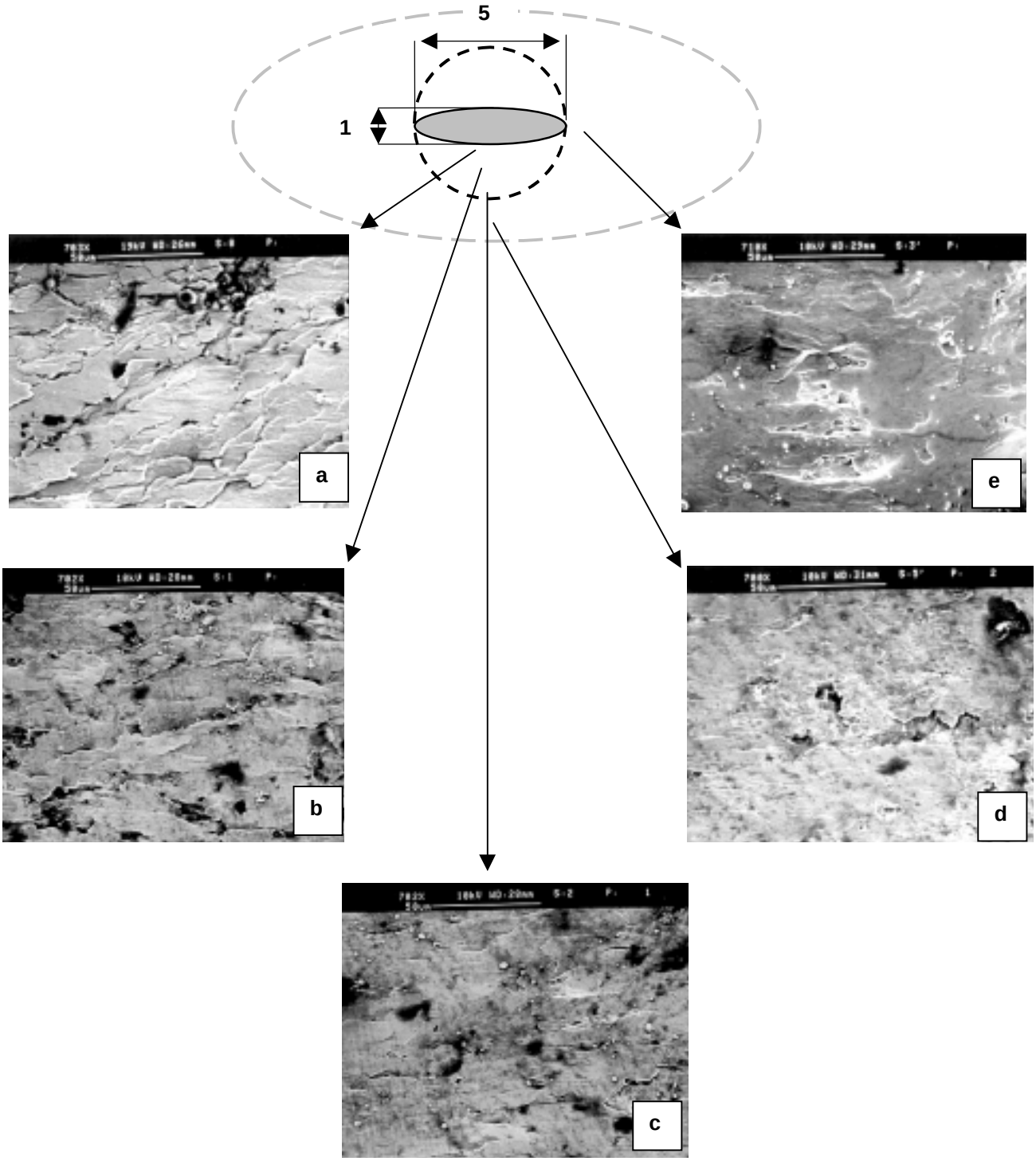

Figure 5: Different crack propagation zone for the 'deep shelling': a) zone close the edge of the original defect; b) fracture at a distance of approx. 1 mm from the defect center; c) zone corresponding to the end of *phase 1*; d-e) fracture surface in the zone corresponding to *phase 2*.

MECHANISMS OF CRACK PROPAGATION

Variable amplitude compression

The first idea that was followed for analysing the mechanism of phase 1 propagation was that the initial stages of propagation are sustained by a mode I propagation. Extensive studies by Suresh and others [14-15] have shown that mode I propagation can occur under compression and crack propagation is amplified by the presence of compression overloads (or 'underloads'). They also suggested that this mechanism could be responsible of crack initiation from deep defects in railway wheel. The other element that is in favour of the hypothesis is that the load spectra of high speed trains, on which the phenomenon of 'deep spalling' is known to occur, are characterised by very high overloads (up to two times nominal loads) on vertical forces [16].

A series of 2-D analyses based on FEM models and Strip Yield models have been carried out considering the average pressure distribution corresponding to a vertical load of 80 kN and an overload pressure corresponding to 1.5 times the pressure caused by nominal loads [17].

The first results of these analyses show that in the compression cycles following the underload the crack tip tends to remain open for a crack advance corresponding to the plastic zone caused by the underload [18] (Fig. 6). Investigation are now being carried out for a precise determination of crack growth under the load spectra resulting from dynamic simulations of the behaviour of high speed trains in different conditions [19].

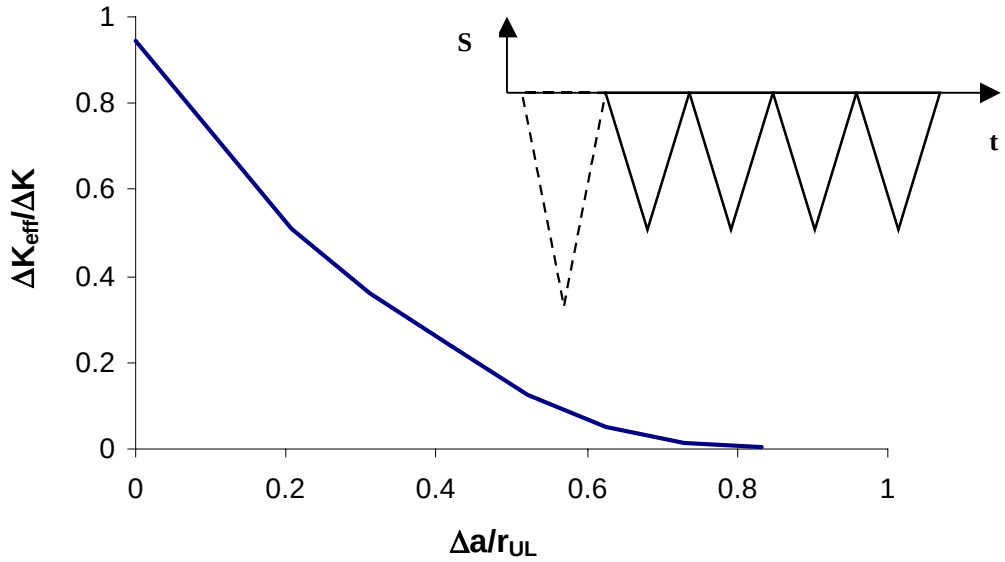

Figure 6: Crack opening ratio for a crack under compression cycles following an underload [17].

A simplified 3-D analysis

On the basis of the results shown in the previous section it is possible to assume that after an underload the crack growing from the initial defect remains completely under the action of compressive loads. It can be so carried out a simplified analysis of the ΔK (mode I, II and III) at the defect, under rolling conditions. The SIFs were evaluated by the stress functions of Irwin [18] and Kassir and Sih [19], considering an elliptical crack in an infinite body subjected to the Hertz stress components under the hypothesis that contact pressure distribution is centered over the crack and that it is moving in the rolling direction. Accordingly (Fig. 6):

$$\Delta K_I = f_I \cdot \Delta\sigma \cdot \sqrt{\pi b} \quad (1)$$

$$\Delta K_{II} = f_{II} \cdot \Delta\tau \cdot \sqrt{\pi b} \quad (2)$$

$$\Delta K_{III} = f_{III} \cdot \Delta\tau \cdot \sqrt{\pi a} \quad (3)$$

where $\Delta\sigma$ and $\Delta\tau$ depend on the depth at which the defect is located.

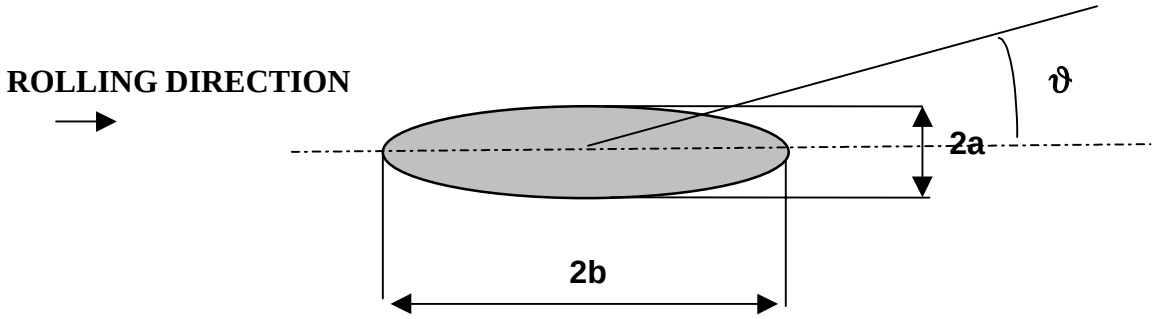

Figure 6: Geometrical description of the initial crack.

In particular stress calculations were carried out with a contact pressure distribution having a maximum Hertz pressure of 850 MPa and a contact area half length along the rolling direction of about 6 mm [19]. The results of the SIF calculations are expressed in terms of a propagation index $P=\Delta K/\Delta K_{th}$. Threshold data for the wheel material are: $\Delta Kth,I,eff$ = 5 MPa√m [20]; $\Delta K_{th,II}$ = 9 MPa√m [13]. Mode III threshold was estimated as to $1.25\Delta K_{IIth}$ on the basis of the results of Hellier, McGirr and Cordering [21] on rail steel. Calculations of the P index for the Fig. 1 defect (2a=1 mm; 2b= 5 mm) are shown in Fig. 7.

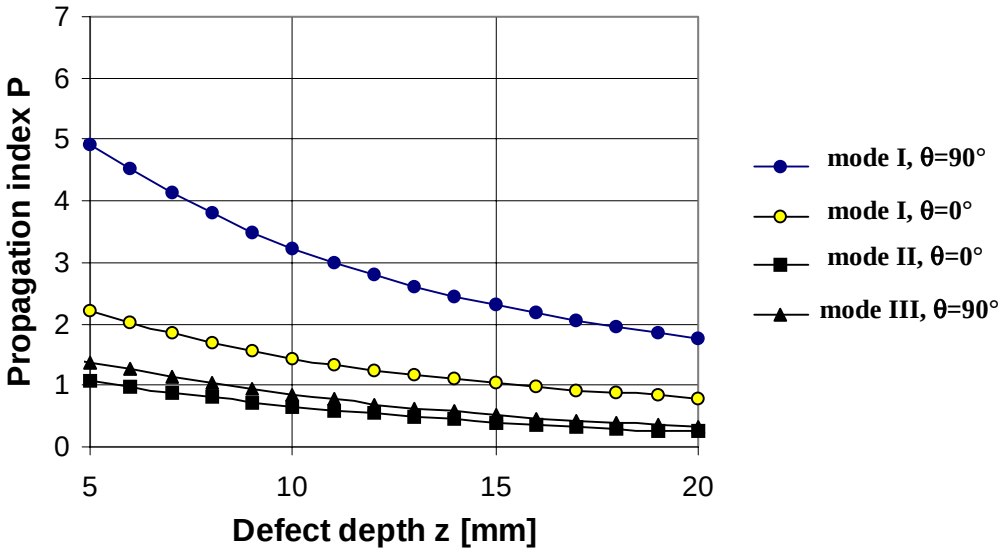

Figure 7: Calculations of the propagation index ($P=\Delta K/\Delta K_{th}$) for a semi-elliptical defect (2a=1 mm; 2b= 5 mm) subjected to cyclic stresses due to rolling contact.

It can be seen from this figure that for a defect depth of 10 mm (that experimentally measured), the only propagation index greater than 1 is that in mode I. It predicts a crack propagation in the transverse direction (ϑ=90°), which is just what happens. However, mode I propagation is able to explain only the initial propagation of the crack, since mode I is suppressed after the crack width is almost twice the initial defect [19] (this is consistent with fractographic observations of Fig. 5).

Nevertheless this initial mode I propagation deeply affects and enhances the subsequent mode II crack growth. After that the crack has changed its initial shape from a/b=0.2 to a/b=0.4-0.5, the mode II geometric factor at θ=90° increases approx. of 100 %.

The graph also shows clearly the influence of the defect depth, which is dramatic in determining its propagation. This fact explains the importance of re-profiling operations, which can activate “sleeping” defects, transporting them towards the surface.

The most interesting point is the fact that acceptance criteria for defects (on new wheels as well as on re-profiled ones) can be based on this initial mode I mechanism, even if this can only be responsible of the first phase of crack growth.

CONCLUSIONS

The mechanism of ‘deep spalling’ has not been completely understood. In this work the propagation mechanism of this kind of deep spalling has been assessed by experimental fractography, statistical analysis of inclusions, simulation of manufacturing process and FEM analysis of crack propagation.
Analyses have shown that the initial stages of propagation are likely to be due to mode I propagation. This mechanism is particularly interesting since it allows to predict the conditions for the onset of ‘deep spalling’ failures.

ACKNOWLEDGEMENTS

This activity are the first results of a research project under the financial support of Lucchini C.R.S.. This support as well as permission to publish results are gratefully acknowledged.

REFERENCES

1. Orringer, O. (1996) *Fatigue Fract. Engng. Mater. Struct.* **19**, 1329
2. Mutton, P. J., Epp, C.J., Dudek, J. (1991) *Wear* **144**, 139
3. Ekberg, A. (1997) Licentiate Thesis, Chalmers University of Technology, Sweden
4. Keer, L.M., Bryant, M.D., Haritos, G.H. (1982), *Journal of Lubr. Techn*. **104**, 347
5. Salehiadeh H., Saka N. (1992) *Journal of Tribology* **114**, 690
6. Lunden, R. (1992) *Proc. International Wheelset Congress*, pp. 163-167, Sydney
7. Melander, A. (1997) *Int. J. Fatigue* **19**, 13
8. Sakae, C., Ohkomori, Y., Murakami, Y. (1999) Technical Report, Kyushu University.
9. Bogdanski, S., Olzac, M., Stupnicki, J. (1996) *Wear* **191**, 14
10. UIC (1984) UIC-Kodex 812-3 V, 5.
11. Murakami, Y., Toryiama, T., Coudert, E.M. (1994) J. testing and Evaluation **22**, 318.
12. M. Faccoli, R. Roberti (2000) Technical Report, Università di Brescia, Dipartimento di Meccanica.
13. Murakami, Y., Fukuhara K. and Hamada S. (2000) unpublished results, Kyushu University.
14. Suresh, S. (1985*) Engineering Fracture Mechanics* **21**, 453.
15. Aswath P.B., Suresh S., Holm D.K., Blom A.F. (1988) *Journal of Engineering Materials and Technology* **110**, 278.
16. Diana, G. Bruni, S., Braghin, R. (2000) Report of Research Contract, Politecnico di Milano, Dipartimento di Meccanica.
17. Lombardo, F., Masanta E. (2000) Graduate Thesis, Politecnico di Milano, Dipartimento di Meccanica.
18. Irwin, G.R. (1962) *Trans. ASME, Ser.E, J Appl. Mech.* **29**, 651
19. Kassir, M.K., Sih, G.C. (1966) *Trans. ASME, Ser.E, J Appl. Mech*. **33**, 601
20. Ghidini A. (1999) Technical report, Lucchini, Lovere.
21. Hellier, A.K., McGirr, M.B., Corderoy D.J.H. (1991) *Wear* **144**, 289.